HydroCen
NORWEGIAN RESEARCH CENTRE FOR HYDROPOWER TECHNOLOGY

CENTRE FOR ENVIRONMENT-FRIENDLY ENERGY RESEARCH

HydroCen Report nr. 38

CFD model simulations for the purpose of optimizing secondary intakes

Application of 3D CFD for intakes, optimization of an existing intake structure

NTNU SINTEF NINA

HydroCen

The main objective of HydroCen (Norwegian Research Centre for Hydropower Technology) is to enable the Norwegian hydropower sector to meet complex challenges and exploit new opportunities through innovative technological solutions.

The research areas include:

- Hydropower structures
- Turbine and generators
- Market and services
- Environmental design

The Norwegian University of Science and Technology (NTNU) is the host institution and is the main research partner together with SINTEF Energy Research and the Norwegian Institute for Nature Research (NINA).

HydroCen has about 50 national and international partners from industry, R&D institutes and universities.

HydroCen is a Centre for Environment-friendly Energy Research (FME). The FME scheme is established by the Norwegian Research Council.

The objective of the Research Council of Norway FME-scheme is to establish time-limited research centres, which conduct concentrated, focused and long-term research of high international calibre in order to solve specific challenges in the field.

The FME-centres can be established for a maximum period of eight years HydroCen was established in 2016.

CFD model simulations for the purpose of optimizing secondary intakes

Application of 3D CFD for intakes, optimization of an existing intake structure

Asli Bor[1]
Marcell Szabo-Meszaros[2]
Kaspar Vereide[1,3]
Leif Lia[1]

[1] NTNU, Vassbygget, Valgrinda, Trondheim, Norway

[2] Sintef Energy, Norway

[3] Sira-Kvina kraftselskap, Norway

HydroCen

Bor, A., Szabo-Meszaros, M., Vereide, K. & Lia, L. 2023. CFD model simulations for the purpose of optimizing secondary intakes. HydroCen report 38. Norwegian Research Centre for Hydropower Technology

Trondheim, september 2023

ISSN: 2535-5392 (digital publikasjon, Pdf)
ISBN: 978-82-93602-39-2

KVALITETSSIKRET AV
Leif Lia

FORSIDEBILDE
Foto: Sira Kvina kraftselskap

NØKKELORD
Brook intakes, CFD, Hydraulic structures, hydropower

KONTAKTOPPLYSNINGER

HydroCen
Vannkraftlaboratoriet, NTNU
Alfred Getz vei 4
Gløshaugen,
Trondheim

www.HydroCen.no

Abstract

Bor, A., Szabo-Meszaros, M., Vereide, K. & Lia, L. 2023. CFD model simulations for the purpose of optimizing secondary intakes. HydroCen report XX. Norwegian Research Centre for Hydropower Technology.

Secondary intakes, also known as brook intakes, are crucial for hydropower schemes in alpine regions with steep hills and a high number of tributaries. Brook intakes are normally a minor part of the total inflow and combined with remote location many brook intakes are left without monitoring or maintenance. Increased focus on loss of water due to rising energy prices now initiates more focus on the performance of the brook intakes. With hundreds of brook intakes in the Norwegian hydropower system, one of the most common types is chosen for further survey; the Tyrolian weir.

CFD modelling of brook intakes are rare due to lack of geometric data and cost of modelling. This project is testing two different types of software to see how modelling can be done in a cost-effective way with scarce input data, and still have sufficient accuracy. Both ANSYS (commercial) and OpenFoam (freeware) are used independently in the project. The geometry is modelled from drone scanning and frow drawings from the construction period. Photos and other observations are used for extra quality control.

From the model both capacity parameters and flow pattern are calculated. For capacity the Cd factor is calculated and compared with literature. Simulated flow patterns through the screen are compared with known reference curves from detailed model studies and observations from full scale. This study is recognized as the first study for Tyrolian weirs with rectangular bars (flat steel) in the rack. Former studies are done with tubes or T-shaped bars.

Both users of ANSYS Fluent and OpenFoam are experienced users of the software, from the research perspective, and their skills are fully comparable. It is found that both the ANSYS Fluent and OpenFoam software gives the same accurate results from the same group of input data. OpenFoam allows a much quicker way through the geometric modelling, where different parts of the model can be separated, and challenges may be overcome more easily. Considering the total simulation times for domains containing approximately the same number of elements and in the simulations with the same parallel computation, modeling with OpenFoam yielded approximately 11% faster results. Other preferences may influence the choice between the models.

It is concluded that the total time consumption for an experienced user is roughly three weeks; one week for modelling, one week for corrections, simulation and experiments and the final week for interpretation and reporting. Of course, with great variation from site to site. In this study, the time spent with the listed procedure was 72 hours and 26 hours, respectively, with ANSYS Fluent and OpenFoam CFD software for a total simulation time of 300 s and 120 s for the domain containing approximately the same number of elements. It is found that the procedure for modelling will be useful for evaluating the performance of brook intakes where water loss is suspected. Further improvements and reduced time consumption will possibly be achieved when modelling a larger number of intakes.

Asli Bor, NTNU Trondheim, asli.b.turkben@ntnu.no
Marcell Szabo-Meszaros, Sintef Energy, Norway, marcell.szabo-meszaros@sintef.no
Kaspar Vereide, Sira-Kvina kraftselskap, Norway, kaspar.vereide@sirakvina.no
Leif Lia, NTNU Trondheim, leif.lia@ntnu.no

Sammendrag

Bor, A., Szabo-Meszaros, M., Vereide, K. & Lia, L. 2023. CFD model simulations for the purpose of optimizing secondary intakes. HydroCen report XX. Norwegian Research Centre for Hydropower Technology.

Bekkeinntak er ein viktig del av eit vannkraftsystem i område med alpin karakter som bratte dalsider, små nedbørsfelt og store trykkhøgder. Bekkeinntak kan gje frå ein liten del (eitt inntak) til ein monaleg del (T.d. Ulla Førre og Svartisen) av den totale avrenninga. Inntaka ligg ofte langt unna kraftstasjonen utan atkomst og overvaking. Høge straumprisar har ført til ekstra fokus på funksjon av bekkeinntak og mulig tap av vatn. I Noreg er det bygd hundrevis av bekkeinntak og den mest vanlege typen er Tyrolerinntak, som også er eksempel i dette studiet.

Computational Fluid Modelling - CFD er ikkje vanleg for bekkeinntak på grunn av manglande geometriske data og kostnaden med å utføre ei slik berekning. Dette prosjektet har testa to ulike programvare for å sjå korleis modellering kan gjennomførast kostnadseffektiv sjølv med avgreinsa bakgrunnsdata, og framleis få tilstrekkeleg nøyaktighet. Det kommersielle ANSYS og gratisprogrammet OpenFoam er brukt til uavhengig modellering. Geometrien er trekt ut frå drone-scanning og frå konstruksjonsteikningar frå byggetida. Foto og andre observasjonar har blitt brukt for kvalitetskontroll.

Med CFD-modellen er bade vanlege kapasitets-parametrar og strøymingsmønster berekna. Cd-faktoren er brukt for kapasitet og den er også samanlikna med anna litteratur. Simulerte strøymingsmønster gjennom rista er samanlikna med nokon kjente referansar med modellstudier og full-skala studier. Dette studiet er så vidt kjent det første studiet der simuleringane er gjennomført med flatt-stål som riststavar. Alle tidlegare refererte studier er gjennomført med T-profil.

Begge brukarane av programvara ANSYS og OpenFoam kan reknast som 'erfarne brukarar', ut ifrå eit forskarperspektiv. Dei vart vurdert til å ha like forutsetningar. Både ANSYS og OpenFoam gjev same nøyaktighet med elles like inngangsdata. OpenFoam gjev rom ei mykje raskare prosedyre for modellering med dårlege geometridata, sidan kvar del kan skiljast lettare frå dei andre. På den måten sorterast problem og feil ut mykje lettare. Berekningshastigheten, dvs. simuleringstida er i gjennomsnitt 11% lågare på Open Foam enn på ANSYS, med elles like data og same tal på element. Personlege ønskje for val av modell kan vektleggast, men det er ikkje gjort her.

Det er konkludert med at totalt tidsforbruk for ein erfaren brukar vil vere om lag tri veker, Ei veke modellering, ei veke med prøvekøyring, korreksjonar, simulering og eksperimentering og den siste veka for tolking og rapportering. Det vil sjølvsagt vere variasjonar frå stad til stad. Det vart gjort forsøk og funnen ei arbeidstid på 72 timar og 26 timar med ANSYS og OpenFoam, respektive. Total simuleringstid var funnen til 300s og 120 s, respektive, med same tal på element i modellen. Med slik modellering er det fullt mulig å finne kapasitet til eit bekkeinntak, og det vil vere til hjelp der du har mistanke om tap av vatn. Sidan dette var eit første forsøk og utvikling av ei prosedyre, er det sannsynleg at tidsbruken vil gå ned når fleire inntak skal modellerast.

Asli Bor, NTNU Trondheim, asli.b.turkben@ntnu.no
Marcell Szabo-Meszaros, Sintef Energy, Norway, marcell.szabo-meszaros@sintef.no
Kaspar Vereide, Sira-Kvina kraftselskap, Norway, kaspar.vereide@sirakvina.no
Leif Lia, NTNU Trondheim, leif.lia@ntnu.no

Content

Foreword

This work has been carried out as an Open Calls project in HydroCen. Reserarchers from NTNU and Sintef has worked together closely to solve the research tasks in the project. The recommendations in the report may be useful for hydropower companies as well as consulting companies delaing with similar issues.

The researchers like to tank Sira-Kvina hydropower company for their great help with providing data to the project. We also like to thank Statkraft who initiated the project and thank goes also to the 'Fagutvalg/Technical committees' in HydroCen who supported and voted for the project in competition with many others.

It is our goal to present the results both in a journal paper and in one or more conferences.

2023-09-26 Asli Bor

1 Introduction

1.1 Motivation

Secondary intakes comprise a significant amount of energy production in the Norwegian hydropower system. In the example of the Sira-Kvina scheme, water corresponding to approximately 800 GWh of electrical energy is collected through such structures. This amount to about 10% of the total produced power from the scheme. If this can be extrapolated to the entire Norwegian power production, about 13 TWh is collected through secondary intakes. At the same time, knowledge about the performance of these structures is limited as instrumentation is seldom installed, and the structures are remotely located with limited inspections.

From a historic perspective all brook intakes are designed to never be the limiting component in the discharge water collection system. The tunnels system has a higher marginal cost and should always be optimized from a marginal cost-benefit calculation, while the brook intake has a low marginal cost, and it is reasonable to ensure excess capacity compared with the tunnel system. Most of the secondary intakes were constructed at the peak of hydropower development in Norway, in the 1960-1980's. Now, after a long period of operation, several of these secondary intakes are experienced to have a suboptimal design. This can simply be too low capacity because of underestimated inflow, or that the intake gets clogged with debris or fills up with sediments and rock material. Issues like side drift, supercritical flow, waves, and aeration are other frequent causes of water spill. In addition, with the current climate change and the increasing frequency and magnitude of floods, more brook intakes may not be optimally designed for the future. As the inlet structure should never limit the intake capacity, the design in such situations should be reconsidered.

Simultaneously, new tools for design and retrofitting of existing brook intakes have become available. These include 3D scanning with drones, 3D drawing programs, and computational fluid dynamics simulations. In combination, these may allow cost efficient mapping of the current situation, and investigation of potential measures to improve and optimize secondary intakes. The motivation of the present work is to investigate the effort in time and cost when applying new tools to investigate measures to improve and optimize secondary intakes.

1.2 Scope of work

The work has been conducted in four stages: (1) screening and definition of two cases-studies. (2) Field work, 3D scanning and collection of documentation of the case-study secondary intakes. (3) theoretical calculations and CFD-simulations of the intake capacity for the two case-studies. (4) evaluation of CFD-simulations as a cost-efficient tool for investigating optimization of existing secondary intakes.

A case study was selected from the Sira-Kvina scheme, the secondary intake Stigansåni, which is constructed as a Tyrolian weir. A photo is presented in this chapter, and additional drawings and photos of the intake can be found in the attachment. This secondary intake is found to have insufficient capacity and periods of water spilling every year. This intake type is selected since it is one of the most typical secondary intake designs in Norway.

The Stigansåni secondary intake diverts water from a 5 km^2 catchment with an annual inflow of 11 mill. m^3. The water is directed into the headrace tunnel of the 960 MW Tonstad power plant and is also utilized in the downstream 150 MW Åna-Sira power plant. The annual production of the diverted water equals about 12 GWh. As can be seen in Figure 1 and 2 the brook intake experience both very dry and very wet conditions. The inflow pattern is sharp with quickly rising floods. Figure 2 shows a situation with water loss, where the intake is saturated, and water is spilling over both the intake rack and also over the concrete weir. This situation occurred during winter, when heavy rainfall was combined with temperature

rise and resulting snow melt. Such events are typical in this region and is observed several times at this intake. The power plant owner is interested in investigating possible measures to increase the capacity of this secondary intake.

Figure 1. *Downstream view of Stigansåni secondary intake during dry conditions.*

Figure 2. *Stigansåni secondary intake during wet conditions.*

1.3 Project background

This project was initiated through FME HydroCen, which is a Centre for Environment-friendly Energy Research (FME) dedicated to research on hydropower. The project was initiated in 2022 through the open calls process, where the main initiative came from Statkraft Energy. The project has had one year of funding with a total budget of 500 000 NOK. The project has been conducted in cooperation between NTNU and SINTEF.

2 Methodology

2.1 Overview

Topographic, geotechnical, and climatic factors directly affect the type of water intake structures that are built. Heavy rain or snowmelt and a large riverbed slope can cause high flow rates, which can prevent, the use of front or side intake structures. Typically, secondary intakes are located remotely without any grid connection or other communication. Their operation is uninterrupted because there are no movable parts or other sophisticated mechanisms in the intake. They simply operate without the need for any intervention, and therefore, little effort is made to introduce control systems or monitor incoming water. Indeed, secondary intakes are normally designed with a discharge capacity large enough to collect all water in normal conditions. That is approximately 10-15 times the mean discharge from the associated catchment. More thorough inspections during excessive flooding, which is become more frequent with the changing climate, may indicate a substantial loss of water for power production. Looking beyond theoretical insufficient capacity, it is necessary to re-assess the capacity of secondary intakes, and when necessary, retrofit some. Loss of water can be caused by one or more of the following:

- Intakes can become clogged due to ice or floating debris
- Many intakes are located in very steep rivers/brooks, and supercritical flow passes the intake lack of dampening in the pool.
- Flow conditions in the intake pool during floods do not sufficiently divert the flow into the intake structure, and water spills over the associated dam crest, mainly from supercritical flood.
- Other components, e.g., side channel, tunnel inlet, and weir inside the tunnel are under-dimensioned/have insufficient capacity.

With the appropriate design of the intake, the quality of the diverted water can be improved by eliminating most of the sediments in the stream. In the design of the structure, it is necessary to consider different aspects. The efficiency of the intake structure depends on several factors, such as the shape of the bars, the net spacing between the bars (void ratio), amount of flow and flow conditions, initial flow depth, and the angle and the length of the rack.

The orifice effect is one of the most important mechanisms in the management of the drawn water in intakes. The height of the water column on the screen directly affects the amount of orifice flow received from the screen. As the screen inclination decreases, the water column height increases. Conversely, decreasing the screen inclination slows the flow velocity over the screen, thus bringing the risk of clogging (Figure 3). The inlets must have the necessary screen inclination to reduce the possibility of clogging. Castillo et. al. (2013) experimented with both sediment-containing and sediment free water and concluded that for sediment-containing tests. The maximum water capturing performances were obtained when the grid slope was 30%, and the worst performance, when 0%. In clean water flow conditions, the maximum performance was obtained at 0% screen inclination, and the worst, at 33% screen inclination. As a result, designs should use the required screen inclination to overcome the clogging problem, but unfortunately, this reduces the water depth in the rack bars, and also, the orifice effect.

There are two main mechanisms that defines hydraulic capacity of inclined intakes: the orifice flow and shear effect. In general, the proportion of directed flow for all orifice structures can be expressed by equation;

$$q_{intake} = \frac{dq}{dx} = Cm\sqrt{2gH}$$

Where; dq/dx is diverted discharge for unit width for length *dx*, *C* is the discharge coefficient, *m* is the void ratio (the ratio of the opening area of the screen) and *H* is the hydraulic head). The orifice equation

has also been expressed as a function of the flow rate and water depth in the water through secondary intake by Garot (1939); Marchi & G. (1947); Bouvard (1953); Nosede (1956b); Mostkow (1957); Brunella et. al. (2003) (Table 1).

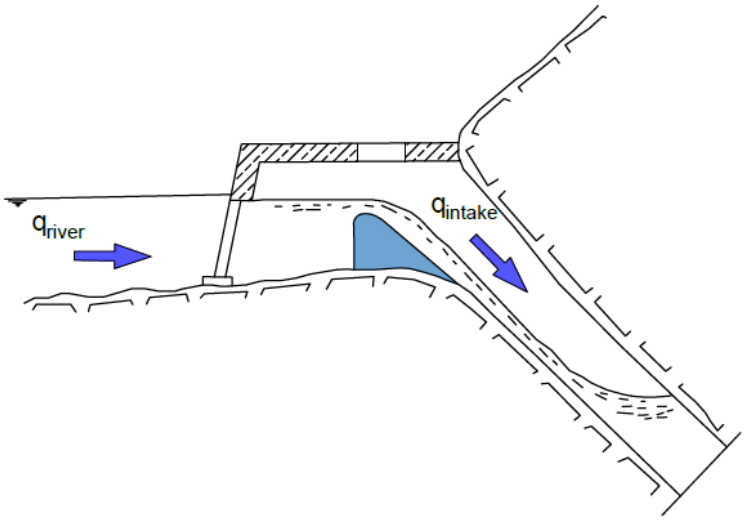

Figure 3. *Definition Sketch of the secondary intake.*

Table 1. *Secondary intake unit discharge equations taken for the study from the literature.*

Researcher	Orifice Equation	*C*
Garot (1939)	$dq/dx = C_d m\sqrt{2gQ}$	C_{d1}
Marchi & G. (1947)	$dq/dx = C_d m\sqrt{2gh_0}$	C_{d1}
Bouvard (1953)	$dq/dx = C_{d0} m\sqrt{2ghcos\theta}$	C_{d1}
Nosede (1956b)	$dq/dx = C_d m\sqrt{2gh}$	$\alpha(D_x/B)^{-0.13}$
Mostkow (1957)	$dq/dx = C_d m\sqrt{2gh_0}$	C_{d2}
Brunella et. al. (2003)	$dq/dx = C_{d0} m\sqrt{2ghcos\theta}$	C_{d3}

Where; C_{d0} is the discharge coefficient calculated under static conditions, Q is the diverted discharge, h is the local flow depth, h_0 is the specific flow depth that is approaching to the rack. C_{d1} is the constant value, but not specified, C_{d2} is in the range of 0.514-0.609 for horizontal racks and 0.441-0.519 for racks inclined at 1/5 slope (suggested by Chardonnet & Meynardi 1954), C_{d3} is measured under static conditions and mainly is mainly affected by void ratio, but also slightly by orifice Reynolds number.

In the literature, the wetted rack length equations required for secondary intakes are theoretically given under two assumptions, the constant energy level approach and the constant energy head approach. In the constant energy level approach, the energy line is parallel to the plane and the energy level line is assumed to be constant, first of all, the water height h and energy height H at the upstream of the grid should be calculated according to the incoming unit flow discharge (q_{river}) (Marchi & G. 1947; Noseda 1956a; Mostkow 1957; Dagan 1963; Krochin & Sviatoslav 1978). The second method for the theoretical approach to secondary intakes is the constant energy head approach. Some researchers in the literature have suggested the wetted rack length using this method (Bouvard 1953; Frank 1956; Brunella, Hager & Minor 2003; Righetti & Lanzoni 2008) (i.e., the energy line is parallel to the rack). In this study, several proposals are selected from the literature to calculate the theoretical wetted rack length L required to obtain a defined flow rate q_1. One of these studies is the study of Frank Von & Erlangen's (1956) method, which is based on constant energy head approach theoretical evaluations and tested with laboratory

experiments. The void ratio, *m*, is computed with the spacing between the rack bars, *b*, and the distance between the middle of two bars, b_w (For Norway, it is normally around $m \cong 0.9$):

$$\boldsymbol{m = \frac{b}{b_w}}$$

The unit discharge *q* and upstream critical depth can be computed with intake width across the river *B*, respectively;

$$\boldsymbol{q = \frac{Q}{B}}$$

$$\boldsymbol{h_c = \sqrt[3]{\frac{q^2}{g}}}$$

The water depth *h* upstream of the rack can be calculated by multiplying the upstream critical depth h_c by the reduction factor *x*;

$$\boldsymbol{h = h_c x}$$

The *x* reduction factor is relative to the angle of the rack and is calculated from the expression below.

$$\boldsymbol{2cos\theta x^3 - 3x^2 + 1 = 0}$$

The minimum length, *l*, of the trash rack required to divert the water at the inlet of the secondary intake structure, is calculated as:

$$\boldsymbol{L = 2.561 \frac{q}{C_d \sqrt{h}}}$$

Where; *C* is the discharge coefficient and is computed from;

$$\boldsymbol{C_d = m\,\mu \sqrt{2gcos\theta}}$$

Where; μ is the contraction coefficient and it depends on the shape of the rack and the flow depth over the rack;

$$\boldsymbol{\mu = 0.8052 m^{-0.16} \left(\frac{b_w}{h}\right)^{0.13}}$$

Other equations taken from the literature for comparison within the scope of this study on the wetted rack length for the secondary intakes are presented in Table 2. It is also used for comparison in the equation used for standard secondary intakes designed in Norway (Bekkeinntak Report, 1986).

Table 2. *Secondary intake wetted rack length equations taken for the study.*

Reference	Wetted Rack Length L (m)
Frank, Von & Erlangen (1956)	$\boldsymbol{L = 2.561\frac{q}{C_d\sqrt{h}}}$
Brunella, Hager & Minor (2003)	$\boldsymbol{L = \left[\frac{0.83h}{C_d m}\right]}$
Drobir (1981)	$\boldsymbol{L = \frac{0.846h}{C_d . m}}$
Bekkeinntak Report (1986)	$\boldsymbol{L = \frac{Q}{C_d . h^{(3/2)}}}$
Where; *L* is the wetted rack length, *h* is the water column height at the beginning of the screen, *m* is the void ratio (the ratio of the opening area of the screen).	

Another parameter that plays an important role in secondary intake design is the discharge coefficient *C*. Many researchers' experimental work has further developed equations for the discharge coefficient (Garot (1939); De Marchi (1947); Noseda (1956b); Frank, Von & Erlangen (1956), Dagan (1963); García (2013)). Researchers have shown that the value of the discharge coefficient depends on certain parameters, in particular, the shape, geometry and spacing between bars are highly effective on the discharge coefficient, as can be seen from the equations and formulas below. The differences between the depth profiles measured and calculated at the head of the rack are caused by consideration of the hydrostatic pressure distribution. The formulas taken from the literature for comparison within the scope of this study are presented in Table 3.

Table 3. *Secondary intake discharge coefficient equations taken for the study from the literature.*

Reference	Wetted Rack Length L (m)
Garot 1939	$\boldsymbol{C_d = \sqrt{\frac{1}{\left(\frac{b_1}{b_1+b_w}\right)^2 \beta \left(\frac{b_w}{b_1}\right)^{\frac{4}{3}}}}}$
Noseda 1956a	For subcritical flow: $\boldsymbol{C_d(h) = 0.66m^{-0.16}\left(\frac{h}{l}\right)^{-0.13}}$ For critical flow: $\boldsymbol{C_d(h) = 0.78\left(\frac{h}{l}\right)^{-0.13}}$
Frank, Von & Erlangen (1956)	$\boldsymbol{C_d(h) = 1.22C_{qh}(h_0)}$

2.2 Numerical modeling with ANSYS Fluent

Real-time observations are the most appropriate for understanding complex real-life rivers, but obtaining such data in the field is very difficult and may even be impossible. Due to the limitations of traditional design methods and models, CFD (computational fluid dynamics) can solve fluid mechanics problems by providing greater quantities of data, and increased profitability, flexibility, and speed compared to experimental procedures. CFD provides the basis for further understanding of the dynamics of multiphase flows, and advances in this area have provided the basis for further insight into the dynamics of multiphase flows. Currently, there are two approaches for the numerical calculation of multiphase flows: the Euler-Lagrange approach and the Euler-Euler approach. Fundamentally, in the Euler-Lagrange approach, the fluid phase is treated as a continuum by solving the time-averaged Navier-Stokes equations, while the dispersed phase is solved by tracking a large number of particles, bubbles, or droplets through the calculated flow field. The dispersed phase can exchange momentum, mass, and energy with the fluid phase, which makes the model inappropriate for modeling of any application where the volume fraction of the second phase is not negligible. In the Eulerian multiphase models, different phases are treated mathematically as interpenetrating continua. The phases can be liquids, gases, solids, or any user-defined

matter and their combinations. The momentum and continuity equations are solved for each phase, and a single pressure is shared by all phases. The parameters obtained from kinetic theory are available, such as shear and bulk velocities, frictional viscosity, or granular temperature …etc.

Laboratory experiments or adequate CFD simulations for secondary intakes are rare because of the complex geometry and high cost of accurate investigations. As mentioned earlier, the efficiency of the intake structure depends on several factors such as the shape of the bars, the net spacing between the bars (void ratio), amount of flow and flow conditions, initial flow depth, and the angle and the length of the rack. Studies in the literature consider a two-dimensional perspective on the vertical plane of the rack. In reality, however, the flow is three-dimensional, and in this case, computational fluid dynamics (CFD) models, once validated against experimental values, can help to better understand the phenomenon (Bombardelli (2012); Blocken & Gualtieri (2012)). However, there are very few studies in the literature modeling the secondary intakes. In addition, different simplifications have been used in these studies. No study has modeled the secondary intake together with the riverbed. While most researchers modeled the water intake structure in one or two dimensions, only a few researchers examined the study in three dimensions (Bombardelli (2012); Castillo & Carrillo (2017); Carrillo et. al. (2018)). Among the studies, there is no study with rectangular bars.

In this study, a numerical model was performed using the Finite-volume schema program ANSYS FLUENT with minimum data from field surveys. For this purpose, easy-to-access remote sensing photos were used as modeling data. The modeling stages includes different phases:

- A high-resolution Digital Elevation Model (DEM) from Google Earth satellite images was used to create the upstream and downstream river terrain of the Stigansåni brook intake area. The DEM file extracted from the satellite images was transferred to the Autocad CIVIL 3D environment, and a 3D triangular model of the riverbed was created as a .stl file.

- The .stl file was opened in the ANSYS Space Claim environment. When created from remote sensing photos, this type of file is generally good quality, but due to the nature of the topography, there may be frequent spikes or missing faces and holes in the terrain. The knit was checked with ANSYS Space Claim and the .stl file was repaired while creating the geometry. The spikes in the field were softened by 40% shrink-wrap and the holes were closed. This approach also facilitates the meshing step, performed in the advanced stages. In fact, the .stl file is simply a location map and is all that is needed for this type of river problem.

- The existing structural project of the Stigansåni brook intake was redrawn in 3D in the CAD environment and the .stl file of the structure was saved separately.

- The structure was added to the river topography prepared in the ANSYS Space Claim environment and the 3D full-scale geometry of the area to be modeled was created. A “fluid domain” of 10m x 10m was defined to represent the riverbed, and the brook intake body was added.

Generating the model geometry is shown in Figure 4.

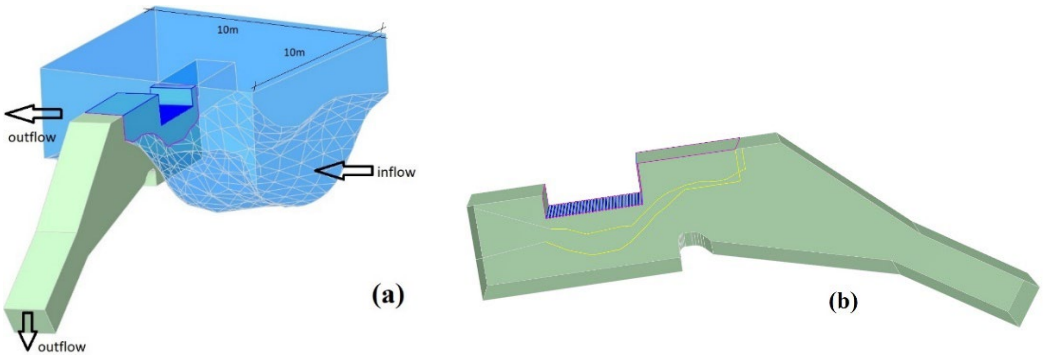

Figure 4. a. Fluid Domain b. Brook Intake

The meshing of the domain is performed via the 'sweep' method for the bottom rack to the brook intake, and the brook intake to riverbed, and the "tetrahedral" meshes for the fluid domain to obtain mesh cells due to the complex geometry (ANSYS FLUENT User's Guide 2021). The generated mesh of the fluid domain consists of approximately 2.8 x 10^6 cells, 13 x 10^6 faces and 8.1 x 10^6 nodes, which means each cell size is small enough when compared to approximate rack grids assigned in simulations. In the simulations, the minimum curvature mesh element size is taken as 1 mm, which is smaller than the rack grid in the brook intake, and this cell size is applied to the denser at the level of the bottom rack. The denser mesh is applied with smaller cell sizes in areas where the brook intake to bottom rack and brook intake to riverbed is densely dispersed through the domain, and the cell sizes are increased towards the edges, to avoid unnecessary mesh density. Regarding the mesh quality of the prepared geometry, the maximum aspect ratio, average skewness and averaged orthogonal quality criteria are calculated as 24, 0.025 and 0.71, respectively. According to the obtained values, the model is considered to have good mesh quality (Figure 5).

In this study, Eulerian multiphase is used to solve the air and water two-phase flow. Air is defined as the primary phase, and water, as the second phase representing the open channel flow. The material properties of both phases are introduced separately, and their densities are taken as 1.225 kg/m^3 and 998.2 kg/m^3, respectively. The surface tension modeling considers the surface tension force as a volume force concentrated at the interface. A surface tension coefficient of 0.072 N/m was specified. No wall adhesion was considered. The viscous flow model is activated with the k-Ω based Shear-StressTransport (SST) model (Menter (1994)) which solved Reynolds-averaged Navier-Stokes (RANS) equations. The time-dependent volume fraction formulation is used, and the volume fraction is obtained with an explicit formulation, such that the Courant number is 0.25 in each time step.

Both phases in the Eulerian flow model were considered as continuous fluids. The sum of the volume fractions (r_α) of the air and water phases is 1 in each control volume. It is 0.5 air volume fraction above the free surface. As for the boundary conditions, the upper river-free surface of the meshed fluid area is simplified as the no-slip wall conditions. The outlet of the river fluid domain and the outlet of the intake structure are defined as the "pressure outlet" boundary condition, with a relative pressure of 0 Pa. This is based on previous flow observations, as the river inlet boundary condition (NVE - The Norwegian Water Resources and Energy Directorate) modeling was conducted by entering the velocity inlet with 4 different flow rates. In addition, the water volume fraction was taken as 1 and the air volume fraction, as 0 in the inlet conditions, and this was simulated. The grid spaces of the intake structure are defined by the "interior" boundary condition between the river fluid domain and the intake fluid domain. Grids, as well as all other outer surfaces (riverbed, riverside surfaces, bottom, up and side surfaces of intake structure), are defined as the no-slip wall conditions (Figure 6).

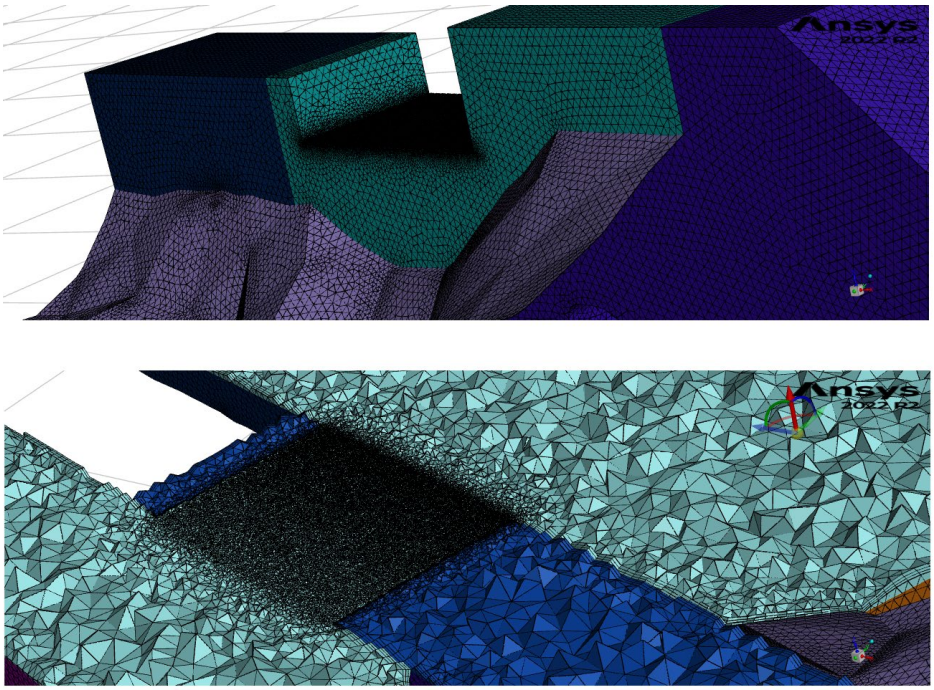

Figure 5. *The computational mesh used in the full-scale modeling using ANSYS Fluent.*

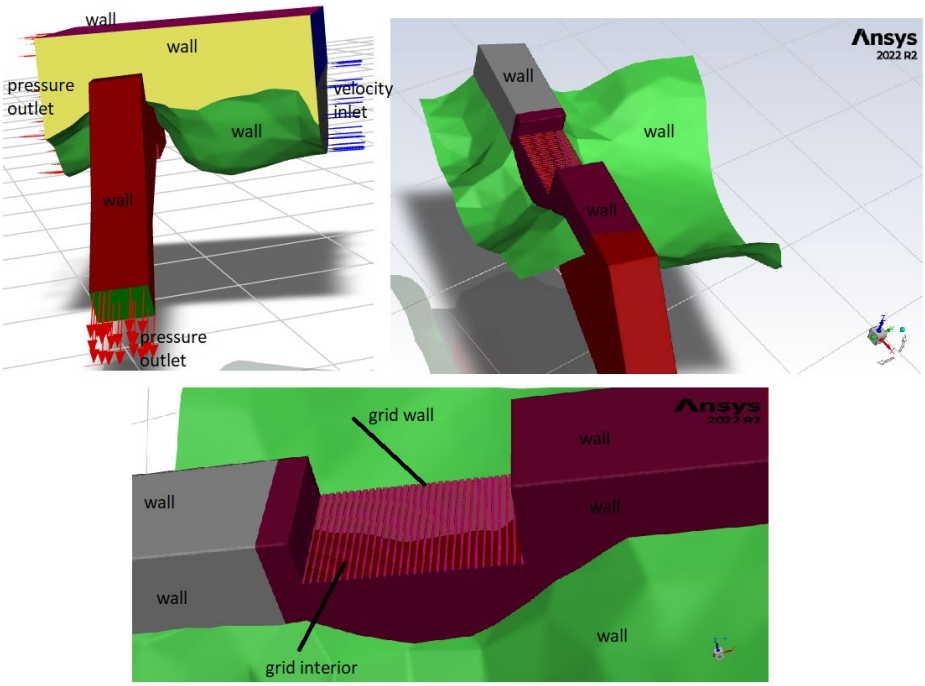

Figure 6. *Boundary conditions used in the full-scale modeling using ANSYS Fluent.*

The simulations were performed in double precision, and as transient flow using the Eulerian multiphase flow model. The solution method of pressure velocity coupling was chosen, combined with the SIMPLEC Scheme. Spatial discretization methods for solving the equation were applied as a second-order upwind scheme to increase the accuracy of the solution. The initial water level in the riverbed was defined by the fluid regions through the domain in the numerical model with the “patch” method in Fluent. The model is simulated for total 300 s with a variable time step of 0.00125 s. CFD simulation took approximately 72 hours for one scenario modelling with running on 32 cores.

2.3 Numerical modeling with OPENFOAM

Similar approach as described in Chapter 2.2 has been applied to test CFD modelling effort and accuracy for the purpose of the project with OpenFoam software (Greenshields, 2018). The main similarities and differences with OpenFoam compared to ANSYS Fluent simulations are described below.

The used method combines Reynolds-averaged Navier-Stokes (RANS) equations with k-ε turbulence model, while the *interFoam* solver was chosen to characterize the free-surface overflow at the Stigansåni intake. The solver utilizes the Volume-of-Fluid approach in order to estimate the water – air boundary layer within each computational cell that are near the simulated water surface.

The simulation domain was defined differently as for modelling with ANSYS Fluent. The upstream end of the OpenFoam domain was set approximately 15 m upstream of the intake structure, while only a few meters downstream of it were covered (in both directions: from the intake tunnel towards to the HPP, and from the downstream part of the watercourse) (Figure 7).

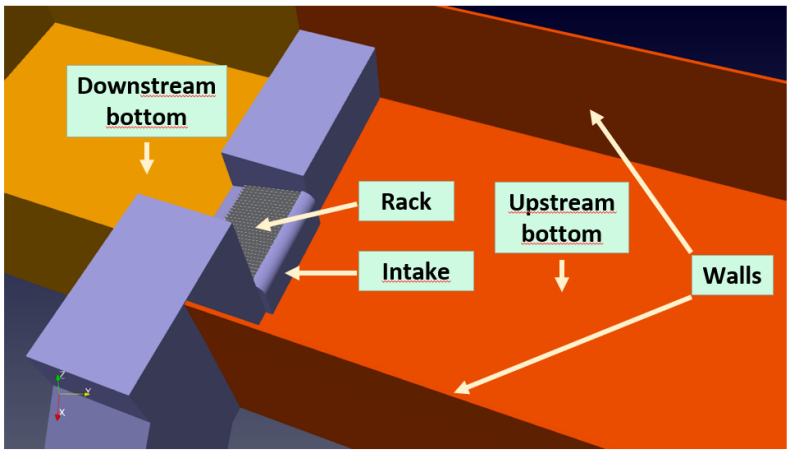

Figure 7. *Defined computational and modelled structures for OpenFoam simulations. Flow direction is from right to left.*

The next difference was in defining the DEM both upstream and downstream of the intake. High-resolution topological survey was available at the area around Stigansåni. At the original bathymetry various polyhedra cell shapes would be generated during meshing process that increase the size of the final computational grid (in terms of cell numbers), and the computation effort (in terms of resources needed to finish a simulation) necessary to achieve converged hydraulic state. However, a simplified topology was used instead. The flow condition over the intake rack structure is estimated to be free-flowing towards the downstream direction without any impact propagated towards upstream (i.e., backed hydraulic jump is not expected to form right over or right downstream of the intake structure, neither any blockage is found at the downstream vicinity of the intake). At the upstream side it needs to be tested how the real topology defines the approaching flow towards to the intake compared to simplified surroundings. For that reason, a comparison analysis was performed between two cases under the same conditions, but with different topology used. The isometric views of the two topologies are presented on Figure 8.

The computational grid was generated with the *snappyHexMesh* utility of OpenFoam. It generates hexahedra-dominant mesh on a user-defined domain. Finer mesh resolution was applied at the intake opening and near the inside weir (Figure 9). Depending on the different setups the mesh size varied between 1×10^6 and 3×10^6 elements.

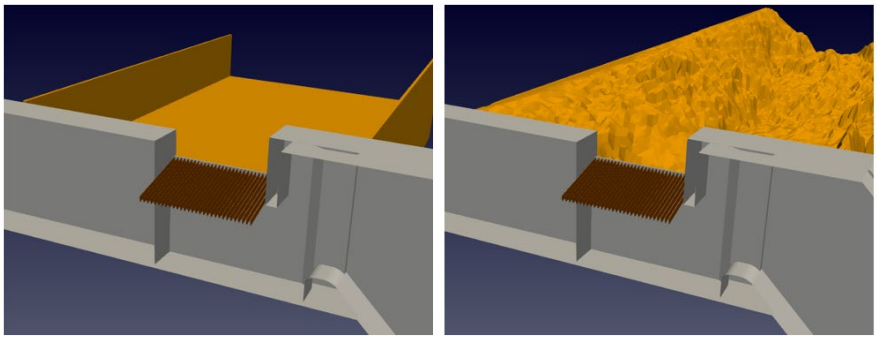

Figure 8. *Modelling domain with simplified surroundings (left panel) of Stigansåni river intake and with measured topology (right panel). Intake structure is presented at the front with the weir inside.*

The modelling strategy with OpenFoam was set on two levels. On the first one the domain was meshed with moderate resolution. In addition, there was no rack structure defined at the intake opening in this case. With such simplifications significant computational effort was spared to initialize the hydraulic conditions at the simulated domain. With a "cold-start" the simulation was set to fill up the upstream reach of the domain with a predefined flowrate (e.g.: Q=4.0 m^3/s) and let it overflow the intake opening. Flowrates were constantly monitored at three patches: inlet, outlet towards the HPP, outlet towards downstream. The first level of simulation was continued until flowrates through the outlets were remained constant over time. Simulated time varied between 80 to 100 s at the first level for the different simulated flowrates. Once hydraulic conditions were developed it was used as an initial condition on the second level of modelling.

On this level the domain that included the intake rack bars was meshed with a finer resolution. The simulation was run further on the finer setup following the same strategy with monitoring the flowrates through the outlets. Based on monitoring the solution it was evident that the intake overflow is fluctuating over time. Upon reaching hydraulic developed state, the simulation was run long enough to determine the statistical average of flowrates through the outlets. That time was set to 20 s and with that it takes 100-120 s in total for simulation of a single case on the two levels.

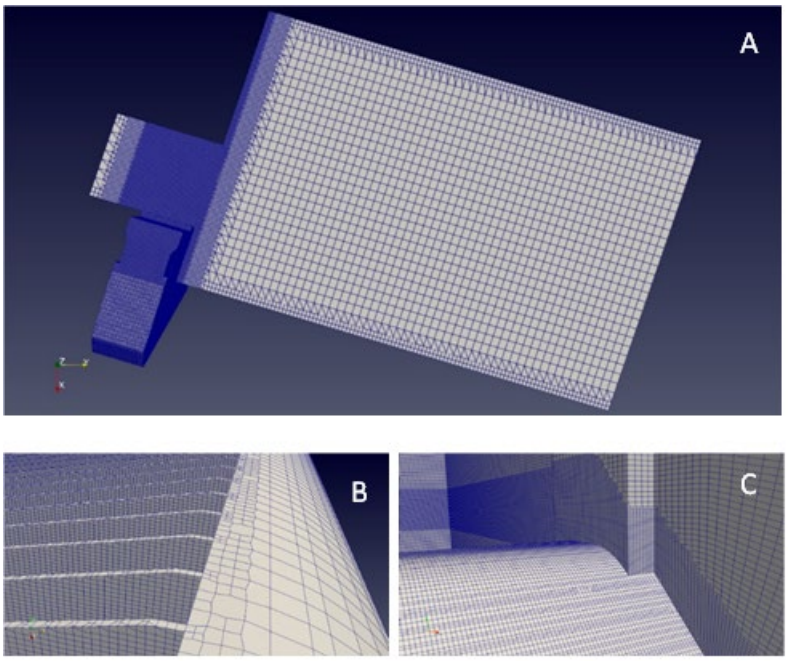

Figure 9. *Generated grid with fine resolution that are applied in OpenFoam. Grid resolution at the domain from the top (panel A), at the upstream end of the rack bars (panel B) and inside the intake with the weir (panel C)*

3 Results and discussion

Simulations were performed with four specific flow rates for Stigansåni brook intake that are selected based on reports from NVE. All flow rates were operated under steady flow conditions of 300 s for ANSYS Fluent and 100-120 s for OpenFoam simulations. The river velocity inlet boundary condition values for each flow rate are given in the table below.

Table 4. *Brook intake discharge coefficient equations taken for the study from the literature.*

Test No	Q (m3/s)	v (m/s)
Q1	3.7	0.18
Q2	5	0.25
Q3	5.5	0.27
Q4	7	0.35
Q is the flow rate; v is the river inlet velocity		

3.1 Flow profile inside of the intake

In Figure 10, the longitudinal flow profiles inside the brook intake for ANSYS Fluent and OpenFoam results can be observed for four specific flows (Q1, Q2, Q3, and Q4), depending on the water volume fraction at 300 s for ANSYS Fluent and 100-120 s for OpenFoam simulations. The 0.5 level of the water volume fraction shows the water levels. In Figure 11, the water levels inside the brook intake for four different flow rates are compared, and it is seen that the values are in harmony.

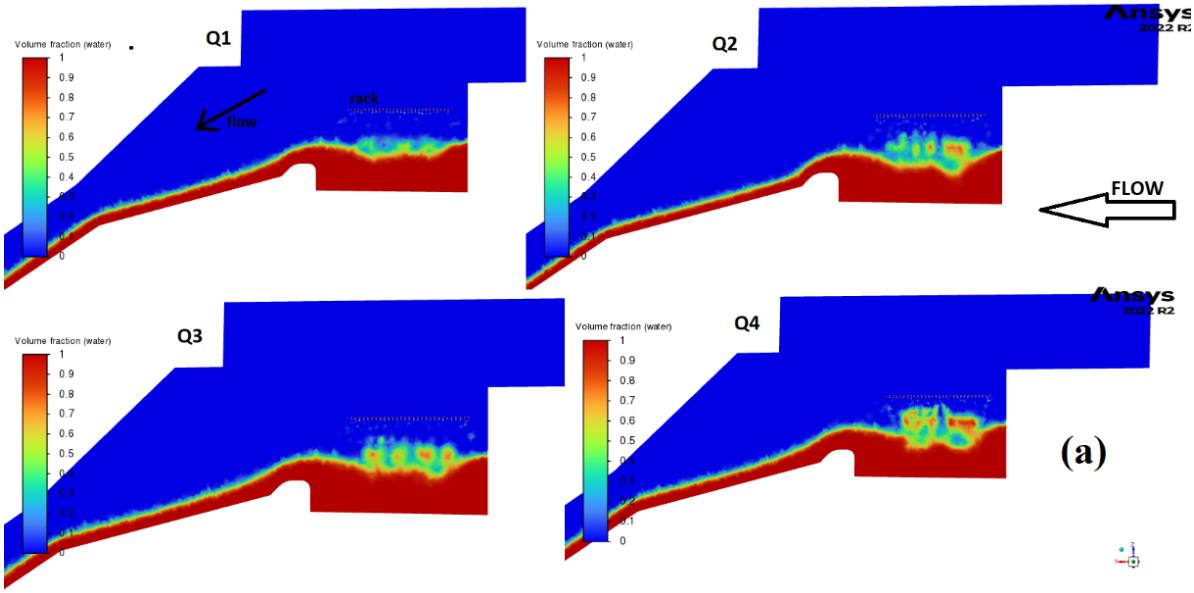

Figure 10. *Variation of water volume fraction inside of the brook intake at a) 300 s for ANSYS Fluent (first four panels) b) 100-120 s for OpenFoam simulations.*

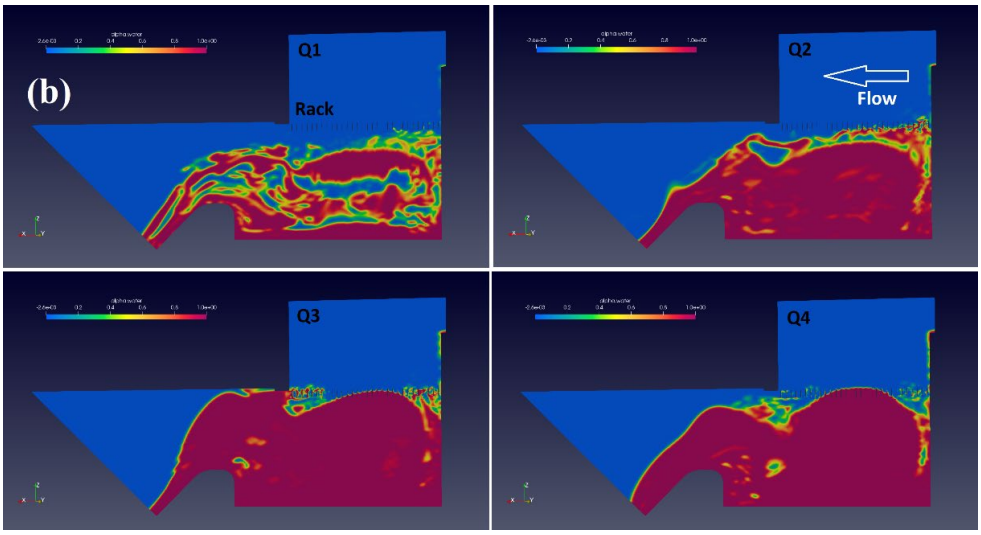

Figure 10. *Variation of water volume fraction inside of the brook intake at a) 300 s for ANSYS Fluent (first four panels) b) 100-120 s for OpenFoam simulations (continued).*

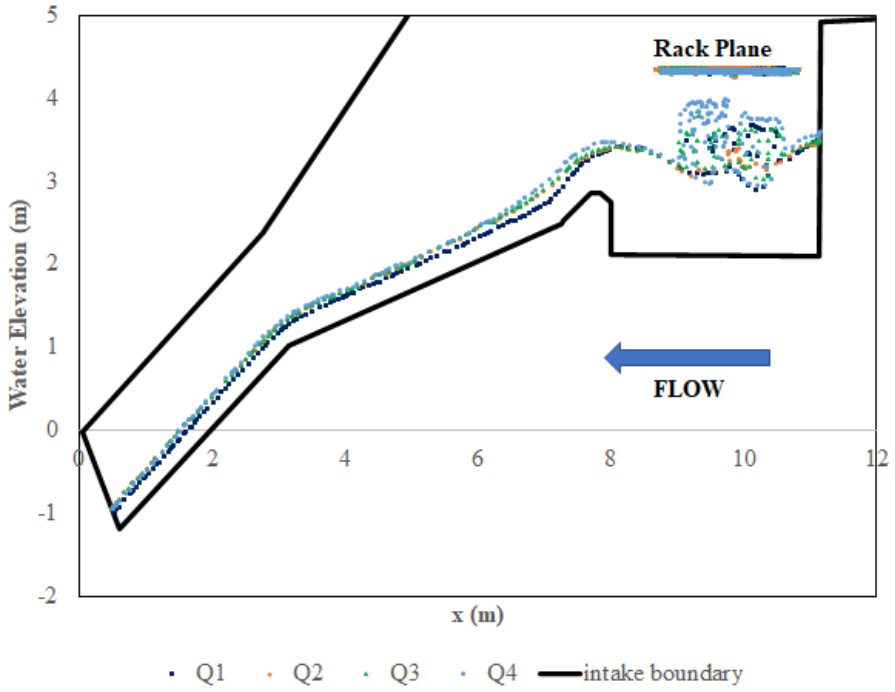

Figure 11. *Flow profiles inside of the brook intake for different flow rates at 300 s obtained ANSYS Fluent.*

3.2 Wetted rack length and flow profile over the rack

In Figure 12, the longitudinal flow profiles over the rack can be observed for four specific flows (Q1, Q2, Q3, and Q4), depending on the water volume fraction at 300 s for ANSYS Fluent and 100-120 s for Open-Foam simulations. The 0.5 level of the water volume fraction shows the water levels. Figure 13 provides a comparison of the water levels over the rack for four different flow rates.

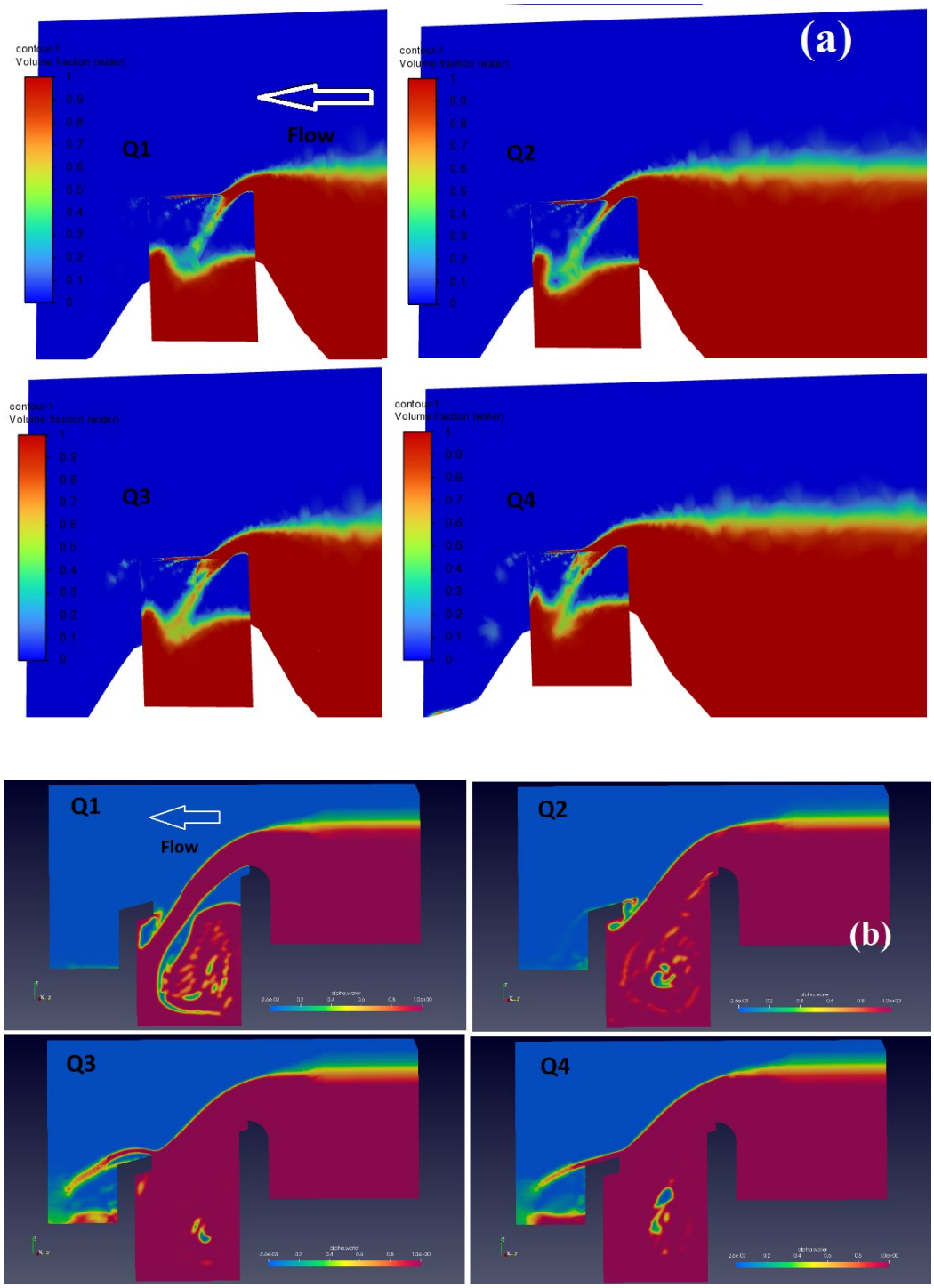

Figure 12. *Variation of water volume fraction over the rack at a) 300 s for ANSYS Fluent (first four panels) b) 100-120 s for OpenFoam simulations.*

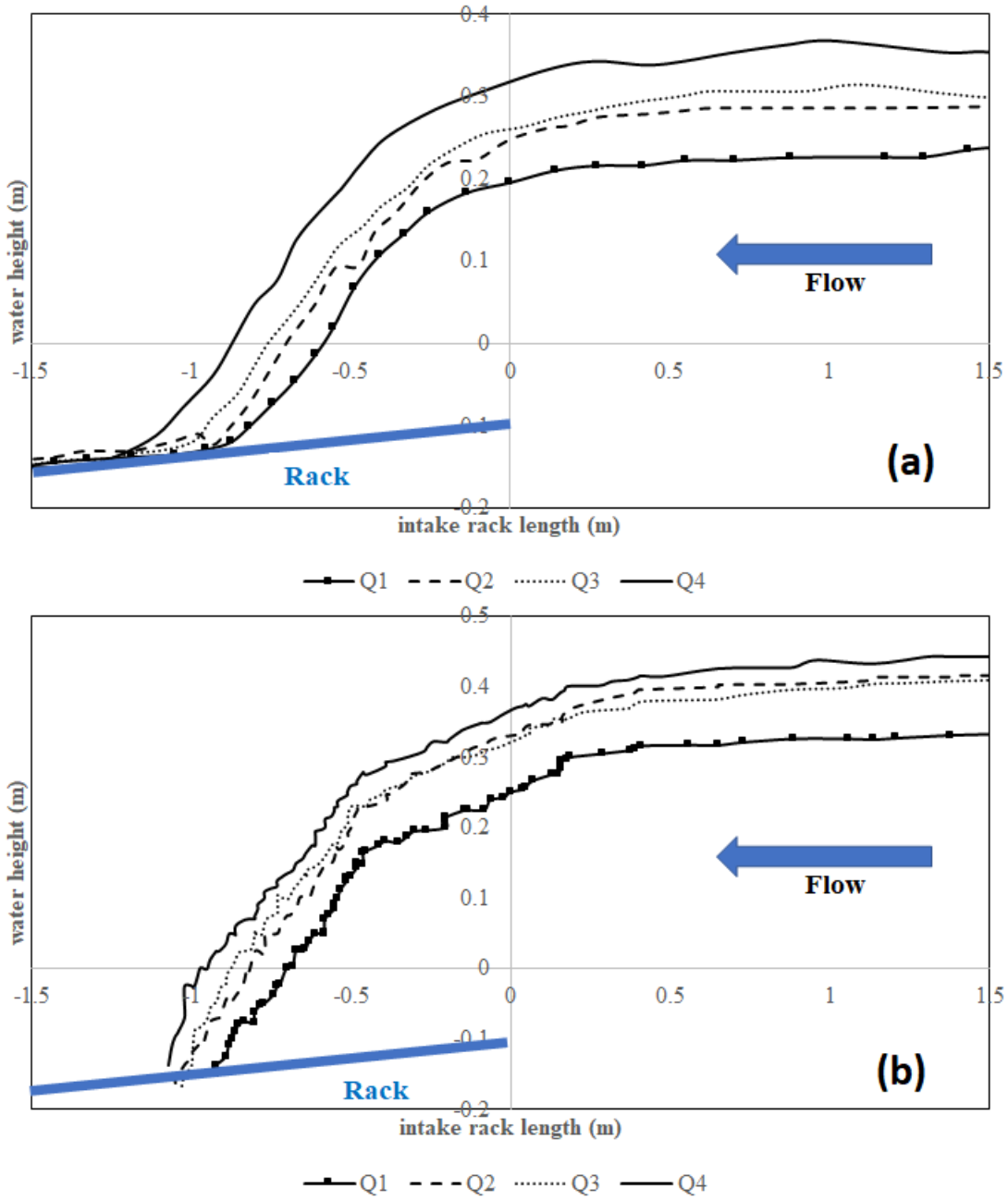

Figure 13. *Flow profiles over the rack at 300 s (a) Ansys Fluent (b) OpenFoam.*

To compare the flow profiles, the water depths were dimensioned using the critical depth h_c, the void ratio m, and the discharge coefficient C_d (Brunella et al. (2003)). Figure 14 shows the dimensionless flow profiles over the rack.

Figure 14. *Dimensionless flow profiles over the rack (a) Ansys Fluent (b) OpenFoam.*

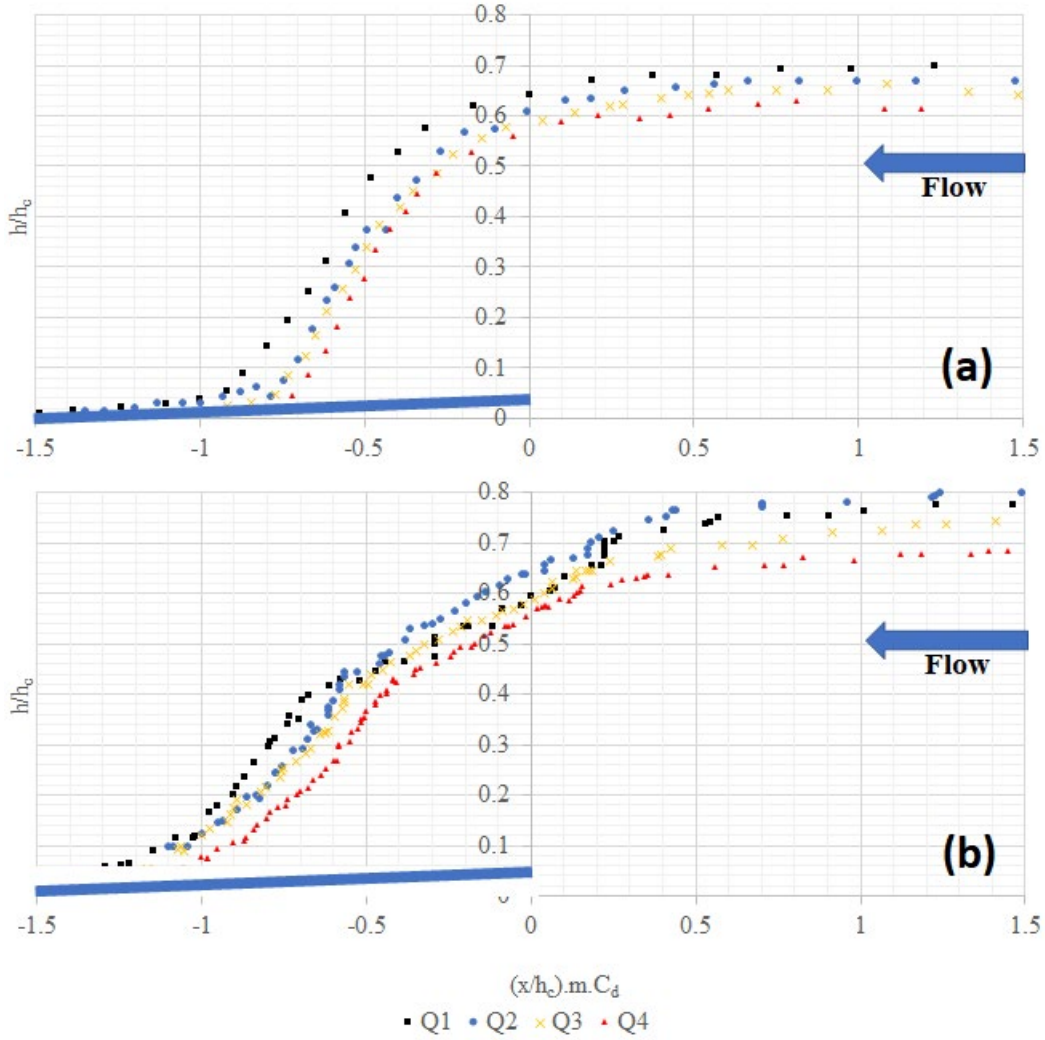

Figure 14. *Dimensionless flow profiles over the rack (a) Ansys Fluent (b) OpenFoam.*

Considering the dimensionless profiles, if we divide into two regions as $x/h_c\ m\ C_d$ >- 0.75 and $x/h_c\ m\ C_d$ <- 0.75 in general (i.e., pre-rack and post-rack), similar behavior is seen for all flow rates. Although the two regions tend to show differences, their behavior can be explained by the following polynomial curve for R^2>0.97 which is similar to that described by Carrillo et. al. (2018);

$$\frac{h}{h_c} = a\left(\frac{x}{h_c} mC_d\right)^4 + b\left(\frac{x}{h_c} mC_d\right)^3 + c\left(\frac{x}{h_c} mC_d\right)^2 + d\left(\frac{x}{h_c} mC_d\right) + e$$

Unlike Carrillo et. al. (2018), model results with OpenFoam showed a logarithmic behavior over bar spacing.

$$\frac{h}{h_c} = a\ln\left(\frac{x}{x_c} mC_d\right) + e$$

Since the pre-rack behaviors of ANSYS Fluent and OpenFoam results were similar, coefficients with R^2>0.91 curve fit were calculated by averaging values. On the other hand, although their behavior over bar and over bar spacing shows the same mathematical expression, the coefficients are calculated sep-

arately because R^2 decreases. Curve fits are R^2>0.99 in this state. The coefficients of the 4th degree polynomial expression obtained for the regions as $x/h_c\ m\ C_d$ >- 0.75 and $x/h_c\ m\ C_d$ <-0.75 and over bar spacing are presented in Table 5.

Table 5. *Coefficients of the mathematical expressions.*

(x/h_c) . m . C_d		**a**	**b**	**c**	**d**	**e**
>-0.75		0.153	0.97	2.06	1.91	0.70
<-0.75 Over Bar		-0.071	0.30	0.42	0.24	0.61
ANSYS Fluent	<-0.75 Over Bar spacing	-0.02	-	-	-	0.11
OpenFoam	<-0.75 Over Bar spacing	0.17				0.31

In order to create a design in which the optimal amount of water is diverted from river, the minimum wetted rack length should be accurately estimated (García et al. (2013)). The minimum wetted rack length was defined by Drobir et al. (1981) as the distance from the beginning of the rack to the section where the nappe enters directly through the racks (measured between the bars) (Figure 10). Figure 14 shows how the discharge coefficient is selected for the brook intakes in Norway, according to Figure 5.7 in the Bekkeinntak Report (1986). Table 2 also gives how the minimum wetted rack length is calculated according to Bekkeinntak Report (1986). When the discharge coefficient C_d is chosen as 2 on the safe side, the minimum wetted rack length is calculated as 2.21 m, which is 2.0 m in the current project. Table 6 shows the comparison of the L_1 values obtained from the numerical simulations and the values calculated from the 3 different equations available in the literature. It can be seen that Frank, Von and Erlangen (1956) equation gives results that are overestimated compared to those from other methods. The results obtained from Ansys Fluent, Brunella, Hager & Minor (2003) and Drobir (1981) methods are very similar. It can be seen that the relationship between flow rate and wetted rack length exhibits a logarithmic behavior (Figure 16).

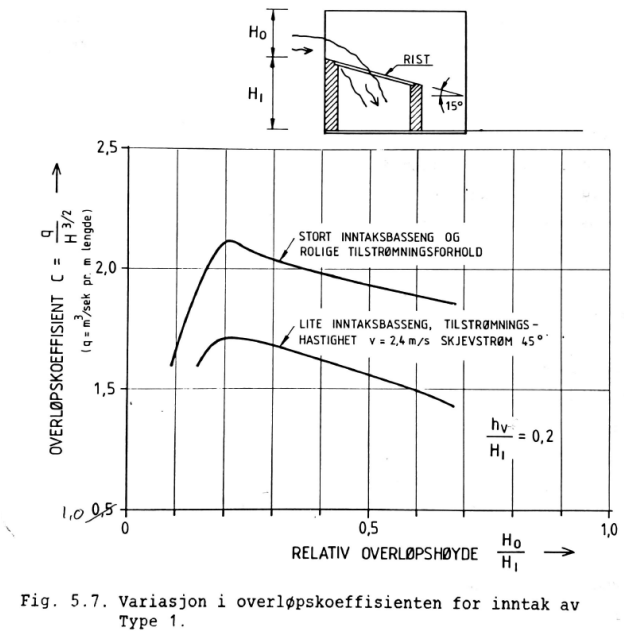

Fig. 5.7. Variasjon i overløpskoeffisienten for inntak av Type 1.

Figure 15. *Variation in overflow coefficient for type1 brook intake.*

Table 6. *Computed Wetted Rack Lengths with various formulas from the literature (units are in meter).*

Q (m^3/s)	L_{1_ANSYS}	$L_{1\_OPENFOAM}$	$L_{1\_Frank\ et.\ al.\ (1956)}$	$L_{1\_Brunella\ et.\ al.\ (2003)}$	$L_{1\_Drobir\ (1981)}$	$L_{1\_Bekkeinntak\ report\ (1986)}$
3.7	0.68	1.07	3.7	0.63	0.64	2.21
5	0.86	1.07	4.64	0.8	0.81	2.21
5.5	0.95	1.38	4.99	0.86	0.87	2.21
7	1.03	1.54	5.98	1.03	1.04	2.21

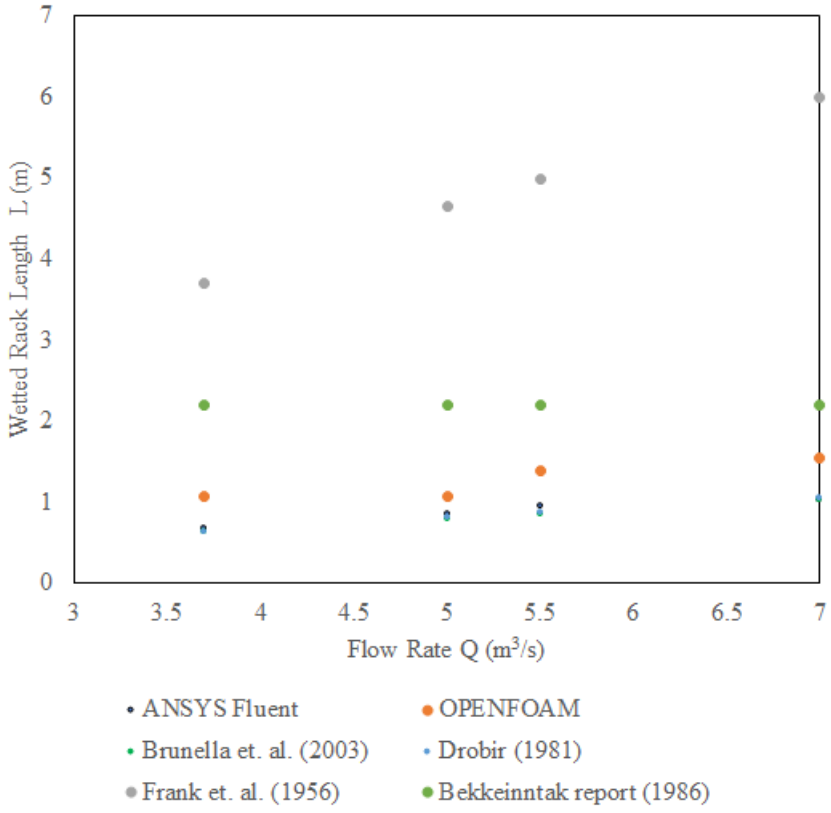

Figure 16. *Change of Wetted Rack Length under different flow rates.*

3.3 Discharge coefficient and water collected

Although, theoretically, the discharge coefficient varies along the rack, formulas presented in the literature generally give average values for each rack. Table 7 shows the discharge coefficient values obtained by Frank (1956), Noseda (1956b) & Garot (1939) equations. Garot's (1939) formula is not flow parameter dependent, and therefore, not affected by flow rate changes, but, for the wetted rack length in the Noseda (1956b) formula, the values obtained with ANSYS Fluent.

Figure 18 shows the dimensionless variation of discharge coefficient across the rack under various flow rates for Stigansåni brook intake. The values obtained from both ANSYS Fluent and OpenFoam were used for the current flow depths. The discharge coefficient changes before and after the rack, and along the rack. In Figure 15, the zero point is the start of the rack and the change after this point is shown for rectangular profiles for Stigansåni brook intake. In the literature, remarkable differences were observed between the behaviors of T-shaped and circular bars (Castillo et al. (2017), Carrillo (2018)). The rack with circular bars has higher discharge coefficients than T-shaped bars. The results of the current research

show that rectangular shaped bars have higher discharge coefficients than circular and T shaped bars. It should be noted that the studies were carried out in clear water conditions without sediment.

Table 7. *Computed Discharge Coefficients with various formulas from the literature.*

Q (m^3/s)	C_{d_ANSYS}	$C_{d\_OPENFOAM}$	$C_{d\_Garot\ (1939)}$	$C_{d\_Noseda\ (1956b)}$	$C_{d\_Frank\ (1959)}$
3.7	1.76	1.55	1.22	0.83	1.31
5	1.63	1.49	1.22	0.83	1.27
5.5	1.57	1.43	1.22	0.84	1.26
7	1.51	1.40	1.22	0.84	1.24

In Figure 17, discharge coefficient values and obtained by Frank (1956), Noseda (1956b) and Garot (1939) equations and numerical results for different specific flows are compared.

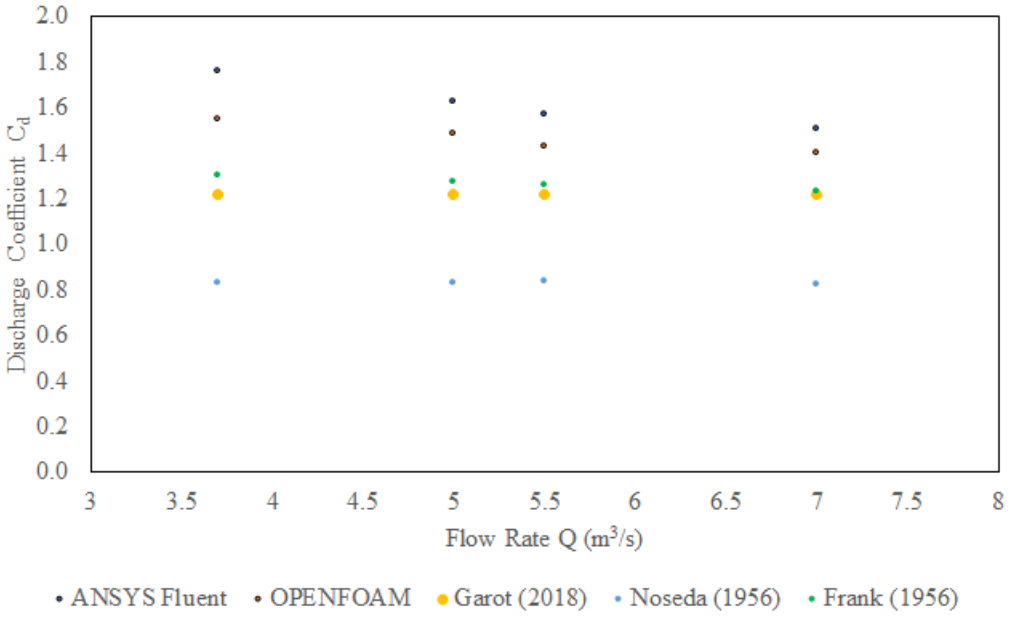

Figure 17. *Comparison of discharge coefficients obtained from variable expressions under different flow rates.*

The behavior of the non-dimensional discharge coefficient in Figure 18 can be mathematically expressed by the following formula for rectangular bars. The *a* and *b* coefficients found for this study are presented in Table 8.

$$C_d = \frac{ae^{b\left(\frac{x}{h_c}m\right)}}{(1+tan\alpha)}$$

Table 8. *Coefficients of the mathematical expressions.*

C_d	*a*	*b*
$C_d = \frac{ae^{b\left(\frac{x}{h_c}m\right)}}{(1+tan\alpha)}$	1	0.046

Depending on the flow rates, the directed water discharges obtained from the model results are presented in the Table 9.

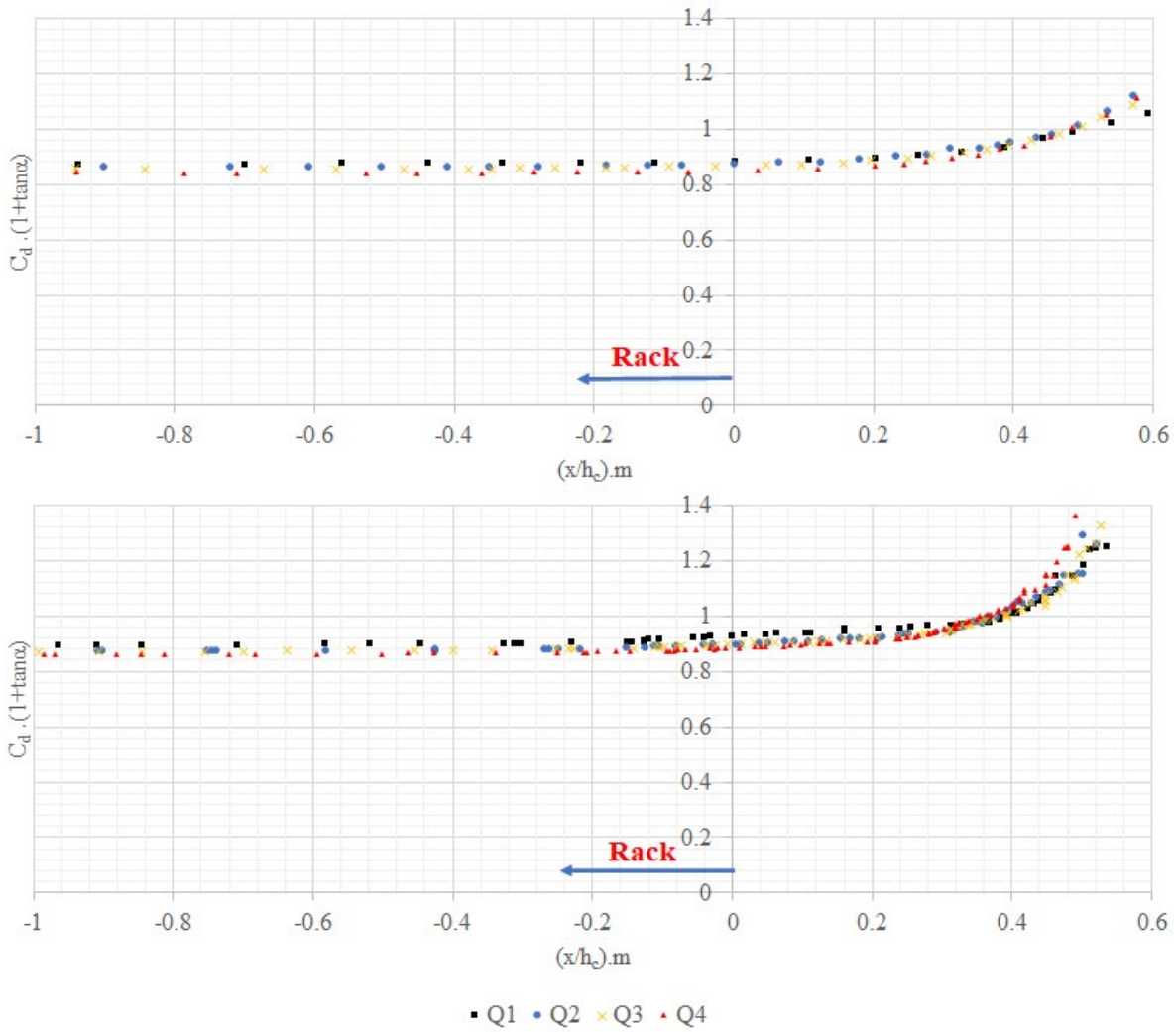

Figure 18. *Variation of the discharge coefficient along the rack for rectangular bars (m= 0.43).*

Table 9. *Flow rate taken into intake calculated with numerical models.*

Q (m^3/s)	Q_{ANSYS} (m^3/s)	Q_{ANSYS} (%)	$Q_{OPENFOAM}$ (m^3/s)	$Q_{OPENFOAM}$ (%)
3.7	3.23	87	3.61	92
5	4.48	90	4.36	88
5.5	4.68	85	4.84	83
7	6.08	87	5.23	76

Marginal difference was spot in simulations with simplified and with real topology tested with OpenFoam. With Q=5.5 m^3/s inlet flow the modelled flowrate averaged over time at the outlet patch towards to the HPP show ca. 3% difference between the two cases (Figure 19). The case with simplified surrounding slightly underestimates the flowrate at the intake outlet, that has been accepted for performing further model simulations on simplified domain.

The water capacity for ANSYS Fluent and OpenFoam numerical models results under different flow rates is presented in Figure 20.
When we look at the results, the water level on the grid and the amount of water collected in the secondary intake structure give approximately the same results with the two models, while the curve behaviors are different from each other. It is seen that curve behaviors are similar to those in the literature

(Castillo & Carrillo (2017); Carrillo et. al. (2018)). On the other hand, this may be due to the large number of meshes. However, the increased modeling time should not be forgotten.

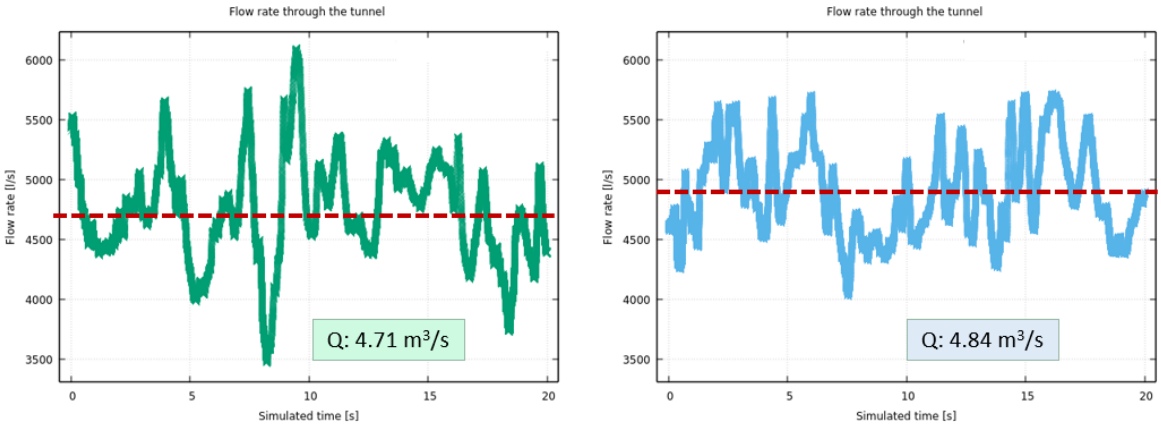

Figure 19. *Simulated flow rate over time at the intake outlet with simplified surroundings (left) and with real topology (right).*

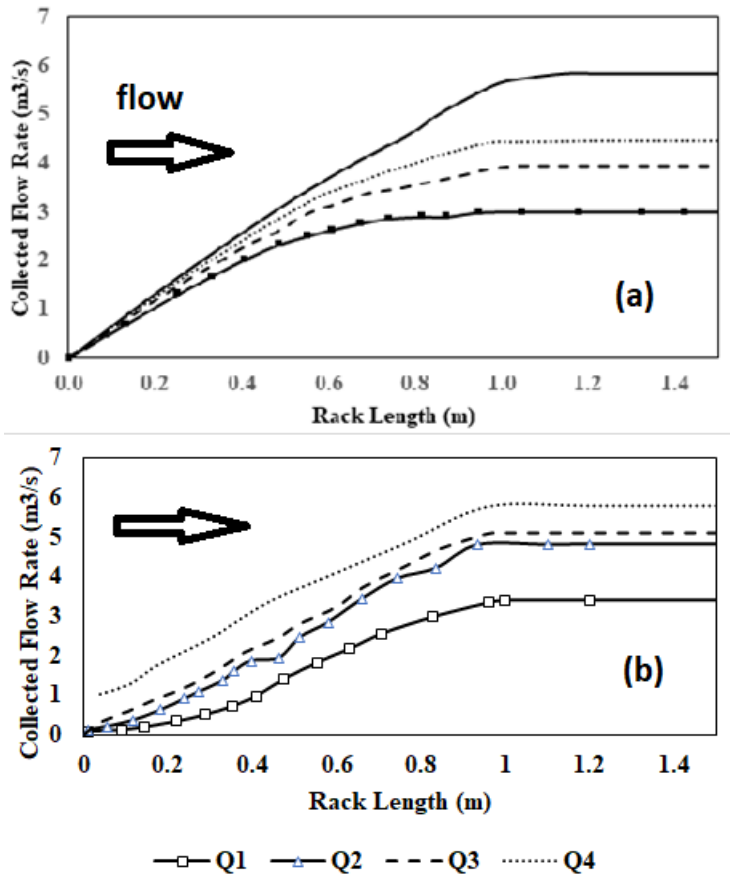

Figure 20. *Water capacity of the Stigansåni brook intake a) ANSYS Fluent b) OpenFoam.*

4 Conclusion

This project is testing two different types of software to see how modelling can be done in a cost-effective way with scarce input data, and still have sufficient accuracy. Both ANSYS Fluent (commercial) and OpenFoam (freeware) are used independently in the project. The geometry is modelled from drone scanning and from drawings from the construction period. Photos and other observations are used for extra quality control. The comparison of the simulation times for the two softwares are given in Table 10. It can be seen that, considering the total simulation times for domains containing approximately the same number of elements and in the simulations with the same parallel computation, modeling with OpenFoam yielded approximately 11% lower simulation times. However, it should be noticed that this speed is increased by the availability of a "cold-start" simulation technique for OpenFoam.

Table 10. *Comparison of ANSYS Fluent and OpenFoam simulation times.*

	Domain Size	Elements	Simulation Time	Paralel Comp.	Computation Time
ANSYS Fluent	10 m x 10 m	2.8×10^6	300 s	32 core	72 h
OpenFoam	10 m x 15 m	$1\text{-}3 \times 10^6$	120 s	32-48 core	26 h

Simulation results showed that:

- In this study, the total time spent for the analysis of an existing structure was approximately three weeks. To model free surface flow and therefore the water intake performance of existing water structures such as secondary intakes, basically all you need is the topographic data (STL file) taken from Drone photographs, you basically don't need anything else. The modeling procedure was found to be useful in evaluating the performance of stream intakes where water loss is suspected.

- According to the studies, the estimation of the flow rate coefficient C_d, which is the design criterion, and accordingly the wet rack length, is the most important parameter that affects the flow rate entering the secondary intake structure. Good calculation of this parameter will provide both economical solution and optimum flow rate input.

- The turbulence models in flow separation have different behavior. In this study, the k-ε turbulence model and the k-Ω-based Shear-Stress Transport (SST) model, which are the most widely used RANS turbulence models in the literature, are used. The results obtained with the tests are almost the same. However, for future studies, different turbulence models should be tested, and the results should be compared.

- An increase in the required wet rack length is expected to collect the same amount of water as clean water.

- It has been observed that the shape of the water profile on the grid in the ANSYS Fluent model prepared using smaller dimensions is closer to the one in the literature.

- In this study, different formulations were applied for rectangular bars. Regarding the coefficient of discharge, rectangular bars have been found to show larger maximum values than T-shaped bars in the literature. This will result in smaller rack length requirements to collect the same flow.

- The results are in agreement with the studies in the literature. An increase in the required wet shelf length is expected to collect the same amount of water as clean water. As such, experiments with sediments are required to know the behavior of the shelves under these conditions.

- The intake structure for a given wet rack length is expected to collect the same amount of water in the presence of sediment material as in clear water conditions. In order to know the behavior of structures in case of sediment transport, bedload simulations must also be performed.

5 References

Blocken, B.; Gualtieri, C. Ten iterative steps for model development and evaluation applied to Computational Fluid Dynamics for Environmental Fluid Mechanics. J. Environ. Model. Softw. 2012, 33, 1–22. 021.
Bouvard, M. Debit d'une grille par en dessous. Houille Blanche. 1953, no. 3: 290-291.

Bombardelli, F.A. Computational multi-phase fluid dynamics to address flows past hydraulic structures. In Proceedings of the 4th IAHR International Symposium on Hydraulic Structures, Porto, Portugal, 9–11 February 2012.

Brunella, S.; Hager, W.; Minor, H.E. Hydraulics of Bottom Rack Intake. Journal of Hydraulic Engineering. 2003, 129, no. 1: 2-10.

Castillo, L.G.; García, J.T.; Carrillo, J.M. Experimental measurements of flow and sediment transport through bottom racks-influence of gravels sizes on the rack. In Proceedings of the International Conference on Fluvial Hydraulics, Lausanne, Switzerland, 3–5 September 2014; pp. 2165–2172.

Chardonnet, E.; Meynardi, G. Étude de grilles pour prises d'eau du type 'en-dessous. La Houille Blanche 1954, 9, 343–351.

Dagan, G. Notes sur le calcul hydraulique des grilles par-dessous. Houille Blanche, 1963, no. 1: 59-65.

De Marchi, G. Profili longitudinali della superficie libera delle correnti permanenti lineari con portata progressivamente crescente o progressivamente decrescente entro canali di sezione constante. Ric. Sci. Ricostr. 1947, 203–208.

Drobir, H. Entwurf von Wasserfassungen im Hochgebirge. Österreichische Wasserwirtschaft, 1981, 243-253.

Frank, J.; Von Obering, E. Hydraulische Untersuchungen für das Tiroler Wehr. Der Bauing. 1956, 31, 96–101.

García, J.T. Estudio Experimental y Numérico de los Sistemas de Captación de Fondo. Ph.D. Thesis, Universidad Politécnica de Cartagena, Murcia, Spain, 2016.

Garot, F. De Watervang met liggend rooster. De Ingenieur in Nederlandsch Indie 1939, 6, 115–132.
Greenshields, C.J., (2018). The Open Source CFD toolbox (Version 8.0). OpenFOAM Foundation Ltd.
Krochin, S. Diseño Hidráulico, 2nd ed.; EPN: Ecuador, Quito, 1978; pp. 97–106.

Mostkow, M. Sur le calcul des grilles de prise d'eau. La Houille Blanche. 1957, no. 4: 569-576.

Noseda, G. Correnti permanenti con portata progressivamente decrescente, defluenti su griglie di fondo. L'Energ. Elettr. 1956a, 33, 41–51.

Noseda, G. Correnti permanenti con portata progressivamente decrescente, defluenti su griglie di fondo. L'Energ. Elettr. 1956, 33, 565–588.

Stokkebø, O., *Bekkeinntak på kraftverkstunneler - Sluttrapport fra Bekkeinntakskomiteen*. 1986, Vassdragsregulantenes forening.

6 APPENDIX

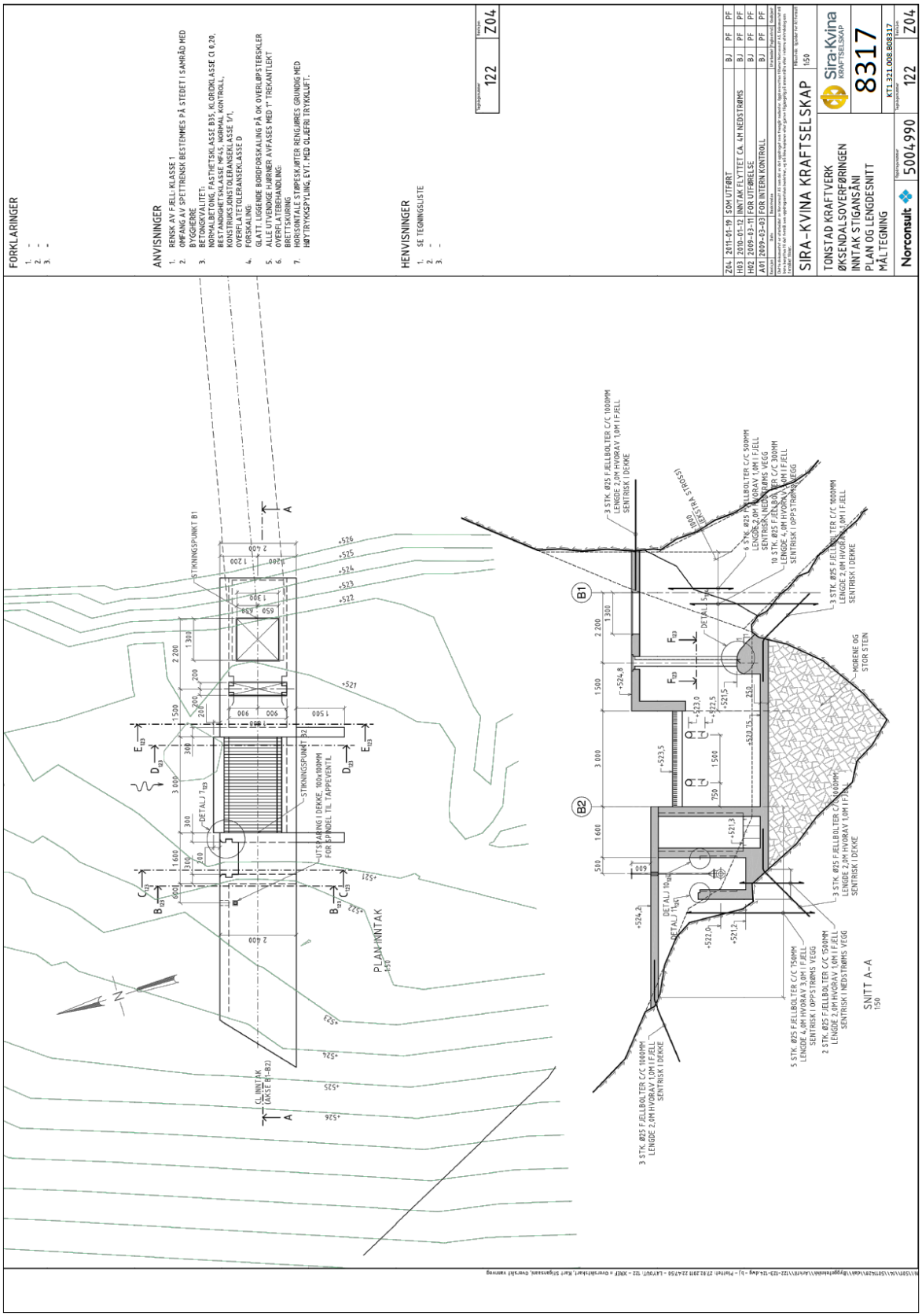

Figure A1: Construction drawings of Stiansåni secondary intake

Picture: Top view of Stiansåni secondary intake

Picture: Side view of Stiansåni secondary intake

Picture: Stigansåni secondary intake during dry conditions

Picture: Stigansåni secondary intake during wet conditions

www.hydrocen.no

ISSN: 2535-5392
ISBN: 978-82-93602-39-2

HydroCen
v/ Vannkraftlaboratoriet, NTNU
Alfred Getz vei 4,
Gløshaugen, Trondheim

www.hydrocen.no
HydroCen
@FMEHydroCen